RPE | Radiation Physics & Engineering
An International Peer-Reviewed Journal
Published by K.N. Toosi University of Technology
http://rpe.kntu.ac.ir
Research Article

Radiation Physics and Engineering 2022; 3(1):21–31
https://doi.org/10.22034/RPE.2022.335096.1061

Removal of Th(IV) ions from aqueous solution using newly developed bi-component bio-based adsorbents

Saeed Alamdar Milani, Ali Yadolahi*, Mohammad Faryadi

Nuclear Fuel Cycle Research School, Nuclear Science and Technology Research Institute, AEOI, P.O. Box: 14893-836, Tehran, Iran

HIGHLIGHTS

- An immobilized hybrid biosorbent (IHB) was prepared for Th(IV) ions removal from aqueous solution.
- RSM was employed for modeling the Th(IV) ions biosorption on IHB.
- The Langmuir maximum monolayer Th(IV) ions sorption capacity of the IHB was found to be 142.86 mg.g^{-1}.
- Th(IV) ions biosorption on IHB followed the pseudo-second-order kinetics model.

ABSTRACT

An immobilized hybrid biosorbent (IHB) was prepared by hybridizing two biosorbents and evaluated for its ability to remove thorium ions from an aqueous solution. The combined effect of the initial pH of the solution (2 to 6), initial Th(IV) ion solution concentration (50 to 300 mg.L^{-1}), IHB dose (0.5 to 5 g.L^{-1}), and sorption duration (10-180 min) were investigated using central composite design (CCD). Experimental data were analyzed using Design Expert 8.0.6 software and fitted to a second order polynomial model with logarithm transform function. The adequacy of the model was verified using three indices, model analysis, coefficient of determination (R^2), and the lack-of-fit test. The initial pH of the solution was determined as the most effectual factor on Th(IV) ions biosorption removal by using the analysis of variance (ANOVA). According to the obtained results, pH value of 4.5, initial metal ion concentration of 210 mg.L^{-1}, IHB dose of 5 g.L^{-1}, and sorption duration of 95 minutes were proven to be the optimum conditions, for maximum biosorption removal of Th(IV) ions from aqueous solutions. Thermodynamic parameters have been evaluated, and it has been determined that the sorption process is feasible in going forward with more products than reactants, exothermic in nature and the reaction is entropy-driven. The equilibrium data were analyzed by the Langmuir, Freundlich, and Temkin sorption isotherms. The maximum monolayer sorption capacity of the IHB was found to be 142.86 mg.g^{-1}. Pseudo-second-order kinetics model provided a better fit for all the biosorption processes which let suppose a physical rate-limiting step for the process.

KEYWORDS

Th(IV)
Sorption removal
Immobilized hybrid biosorbent (IHB)
RSM
Sorption isotherm

HISTORY

Received: 27 March 2022
Revised: 15 April 2022
Accepted: 19 April 2022
Published: Winter 2022

1 Introduction

Thorium is a natural radioactive element (radioelement) widely distributed over the earths crust with nuclear significance. In the development of nuclear energy, thorium is considered a potential substitute for uranium in nuclear power generation facilities (Herring et al., 2001). The toxic nature of this radionuclide, even at trace amounts, has been a serious public health problem for many years (Choppin, 2003). Toxic heavy metals, whether radioactive or not, which are released by many industrial activities, mines and mining plants, are well-known environmental pollutants due to their toxicity, persistence in the environment, and bio-accumulative nature (James et al., 2009). Thorium not only has chemical toxicity as do other heavy metals, but also has radioactivity. It is, therefore, necessary to give particular attention for removal of thorium ions from different effluents. Hence, several techniques have been investigated for heavy metals removal from aqueous solutions and wastewaters and these include chemical precipitation (Kimura and Kobayashi, 1985), ion exchange (Kiliari and Pashalidis, 2011), liquidliquid ex-

*Corresponding author: Ayadollahi@aeoi.org.ir

traction (Bayyari et al., 2010), membrane processes (Ilaiyaraja et al., 2015) and adsorption/sorption (He et al., 2007). Among them, the adsorption technique is probably the most attractive process because it is a more efficient, simple, versatile, cost-effective, and best-suited process for the removal of for heavy metals removal from aqueous solutions (Guerra et al., 2009), despite the cost of the substrate and its regeneration which are concerned as limiting factors (Petrus and Warchoł, 2003). Therefore, it becomes of importance to search for low cost substrates as alternatives or complements to activated carbon and resins. Biosorption represents a more favorable alternative to replace the extant technique for Th(IV) removal from industrial wastewater using biological material and their chemical treatment products. The principal benefits of this technique are the recyclability of biomaterial, low operating- expense, better selectivity for particular metals of interest, removal of heavy metals from wastewater, regardless of toxicity, small operation time, and free from secondary compounds production which might be toxic (Mungasavalli et al., 2007; Srinath et al., 2002).

Over the past few years, immobilized organisms have been increasingly used in batch and continuous experiments. The immobilized organism technology offers some advantages over the use of freely-suspended cells, e. g. ameliorated sorption capacity, reasonable ability to revitalize and separate the biomass from bulk liquid, high biomass loadings, minimal clogging in continuous flow systems (Hrenovic et al., 2012; Wahab et al., 2009), good particle size control is possible, and high flow rates with or without recirculation can be achieved. Moreover, the uncomplicated operation of reiterated biosorption-desorption cycles with immobilized biomasses makes the biosorption process potentially more economic and competitive (Akar et al., 2009; Bağ et al., 1998).

In this study, the sorption potential of IHB for the biosorption of Th(IV) ions from an aqueous solution was investigated. Various important parameters like IHB dose, Th(IV) ions initial concentration, sorption duration, and pH of the metal ion solution were optimized by using a central composite design in response surface methodology (RSM). The traditional one-factor-at-a-time (OFAT) approach for the determination of optimized conditions for different parameters is not economical but is both costly and time consuming due to the requirement of the higher number of experiments, whereas the design of experiments (DOE) for the media optimization in biosorption process can overcome the limitations of traditional OFAT method and can be a powerful tool for the optimization of Th(IV) removal from aqueous solution. DOE requires fewer experiments, lesser time, and lesser material to obtain the same amount of information (Gusain et al., 2014). Sorption removal of Th(IV) onto the IHB has been evaluated in terms of equilibrium, kinetics, and thermodynamics studies. The isotherm models such as Langmuir, Freundlich, and Temkin isotherm models have been used to describe the equilibrium data. Kinetic data obtained from the batch sorption studies were fitted to pseudo-first order, pseudo-second order equations, and intraparticle diffusion models.

2 Material and Methods

2.1 Materials

All chemicals and reagents were used as received without further purification. Milli-Q water (resistivity of 18.2 MX.cm) was used in all designed experiments. A thorium bulk stock solution containing 1000 mg.L^{-1} of Th(IV) was prepared by dissolving 2.457 g of $Th(NO_3)4.5H_2O$ (supplied from Merck, Darmstadt, Germany) in 1% nitric acid, and diluting to 1000 mL using pure distilled water. The standard working solutions were prepared daily from stock solutions. The sample of Cystoseira indica, red marine algae (seaweed), was hand collected from Oman's sea (Iran). Bakers yeast, Saccharomyces cerevisiae, was supplied by a grocery shop. Silica gel 60 Å, 0.063 to 0.200 mm (70 to 230 mesh ASTM) was used as support.

2.2 Instrumentation

Thorium ions concentrations were determined by PerkinElmer Optima 2000 DV ICP-AES. The batch sorption experiments were conducted using a thermostated shaking water bath GFL-1083 Model. The solution pH was measured by a pH meter (Metrohm 780 Model). A NAPCO 2028R centrifuge was used for the centrifugation of the samples.

2.3 Preparation of immobilized hybrid biosorbent (IHB)

For the sorption removal studies, the collected fresh macro algae samples were rinsed with tap water (TW), and washed extensively with distilled water to remove the unwanted materials, dirt and salts (potassium, magnesium, sodium and calcium). The washed algae were then dried in an oven at 70 °C for 24 h. The dry biomass was powdered and sieved using a British Standard 120 mesh ($<$ 250 μm) sieve. Powdered material was preserved prior to use in the biosorption study.

The immobilization procedure was adjusted by (Mahan and Holcombe, 1992). The Cystoseira indica algae, bakers yeast Saccharomyces cerevisiae and silica gel were used to prepare an immobilized hybrid (IHB) biosorbent for the sorption removal of thorium experiments as described below. The IHB was prepared considering the approach proposed by (Bağ et al., 1998) and (Donat and Aytas, 2005) for the immobilization of microorganisms. Dry Cystoseira indica algae biomass powder (20 mg) and baker's yeast Saccharomyces cerevisiae (50 mg) were mixed with 500 mg of silica gel. The mixture was soaked in deionized water and vigorously mixed. After mixing, the paste was dried at 105 $\pm$ 2 °C in an oven for 2 h. The soaking and drying step was repeated to maximize contact between Cystoseira indica algae, Saccharomyces cerevisiae and silica gel and to improve the immobilization efficiency. Then the IHB was sieved through $<$ 250 μm. The IHB was then dried in an electric oven at 70 °C for 24 hours before being used for the sorption removal experiments and the powder was stored in a desiccator.

Table 1: Coded and actual levels of four variables.

Factors	Initial pH (A)	Sorption duration (B) (min)	Initial concentration (C) ($mg.L^{-1}$)	Biosorbent dose (D) ($g.L^{-1}$)
$-\alpha = -2$	2	10	50	0.5
-1	3	52.5	112.5	1.63
0	4	95	175	2.75
+1	5	137.5	237.5	3.88
$+\alpha = +2$	6	180	300	5

2.4 Experimental design

A three-level- four-factor (43) central composite design (CCD) was adopted to optimize conditions for the sorption removal of thorium from aqueous solutions. Initial pH (A), sorption duration (B), initial Th(IV) ions solution concentration (C), and biosorbent dose (D) were the independent process variables considered while sorption capacity of the IHB for metal ions (q) was taken as the response variable. The coded and actual levels of the independent variables are given in Table 1. The levels of RSMindependent variables for the Th(IV) ions removal were determined based on the preliminary experiments. 24 experiments, augmented with six replicates at the center points to evaluate the pure error were carried out in triplicate. The actual experimental design matrix is given in Table 2. After performing the experiments, the response variable (percentage biosorption) was fitted with a second-order model to correlate the response variable to the independent variable (Janin et al., 2009). The common form of the quadratic polynomial equation is as follows:

$$Y = \beta_0 + \sum_{i=1}^{k} \beta_i x_i + \sum_{i=1}^{k} \beta_{ii} x_i^2 + \sum_{i=1} \sum_{j=i+1} \beta_{ij} x_i x_j + \varepsilon \quad (1)$$

where Y is the response (dependent variable) denoted as the predicted sorption capacity of IHB for Th(IV) removal, β_0 the constant coefficient (model intercept), β_i, β_{ii}, and β_{ij} the coefficient for the linear, quadratic and combined effect, k the number of factors studied and optimized in the experiment, x_i and x_j the factors (independent variables), x_i^2 is the square effect, $x_i x_j$ is the combined effect and e stands for the error. The actual experimental design matrix is given in Table 2. The validity of the model was expressed in terms of coefcients of determination (R^2), and the sufficiency of the model was further evaluated by analysis of variance (ANOVA) and lack-of-fit test. The software 'Design Expert' (Ver.8.0.6, from State-Ease Inc., MN, USA) was utilized for graphical analysis and regression of the experimental data.

2.5 Batch equilibrium experiments

The batch sorption removal experiments were carried out by mechanically shaking (200 $r.min^{-1}$) 100 mL of thorium aqueous solution with different pH, initial metal ion concentration, biosorbent dose, and for different sorption duration, at 25 °C. The solution was separated from the solids by centrifugation (for 5 min at 4000 $r.min^{-1}$). The concentration of thorium in an aqueous solution was determined spectrometrically by ICP-AES as mentioned earlier (Niedzielski and Siepak, 2003). The amount of removed thorium ions was calculated from the difference of the thorium concentration in an aqueous solution before and after biosorption removal. All sorption experiments were carried out with three repetitions, and the average value was reported. The responses were recorded in the form of sorption capacity ($mg.g^{-1}$) and percentage biosorption of Th(IV) ions using the following equations:

$$q_e = (C_i - C_f) \times \frac{V}{m} \quad (2)$$

$$\text{Biosorption}(\%) = \frac{C_i - C_f}{C_i} \times 100 \quad (3)$$

where C_i and C_f are the initial and the nal concentrations of the metal ion solutions ($mg.L^{-1}$), respectively. V is the volume of the solution (L), and m is the mass of the biosorbent (g).

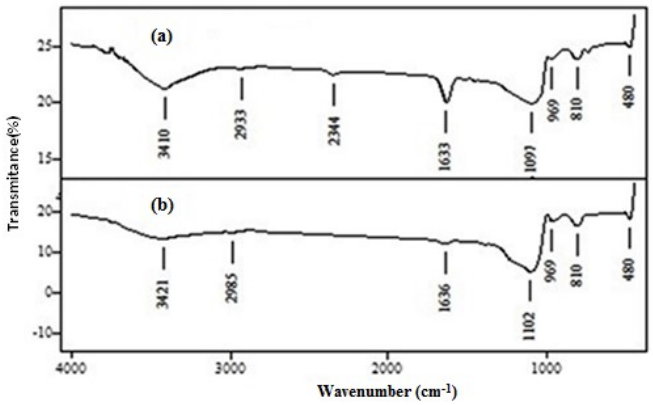

Figure 1: FTIR spectra of the IHB (a) before and (b) after Th(IV) sorption.

3 Results and Discussion

3.1 Characterization of immobilized hybrid biosorbent (IHB)

Infrared (IR) spectroscopy characteristics in the range 400 to 4000 cm^{-1} (Fig. 1) were recorded before and after sorption to determine the main functional groups of the IHB. The characteristic peaks can be assigned to the main functional groups involved in the biosorption by analyzing the

Table 2: Design matrix for CCD and average measured percentage biosorption of Th(IV) ions.

Run order	Independent variables				Biosorption (%)	
	Initial pH	Sorption duration (min)	Initial concentration ($mg.L^{-1}$)	Biosorbent dose ($g.L^{-1}$)	Experimental	Predicted
1	4	95	175	2.75	73.06	74.15
2	4	95	175	2.75	73.11	74.15
3	4	95	175	2.75	76.93	74.15
4	4	10	175	2.75	34.83	36.99
5	4	95	175	2.75	72.39	74.15
6	5	137.5	237.5	1.625	69.01	66.95
7	4	95	175	0.5	39.87	42.75
8	5	52.5	237.5	3.875	65.48	63.13
9	4	95	300	2.75	48.83	54.36
10	4	95	175	2.75	76.97	74.15
11	5	52.5	112.5	3.875	71.47	74.58
12	4	95	175	5	99.97	94.97
13	4	180	175	2.75	85.41	81.92
14	2	95	175	2.75	26.16	26.05
15	5	137.5	237.5	3.875	89.48	89.89
16	3	137.5	237.5	3.875	61.74	62.75
17	5	137.5	112.5	3.875	96.32	98.10
18	3	137.5	112.5	3.875	68.02	71.80
19	4	95	175	2.75	72.57	74.15
20	3	52.5	237.5	3.875	44.34	42.59
21	4	95	50	2.75	76.85	79.47
22	3	52.5	112.5	1.625	32.46	31.88
23	6	95	175	2.75	60.16	61.53
24	3	52.5	112.5	3.875	51.44	52.76
25	5	137.5	112.5	1.625	76.94	79.02
26	3	137.5	237.5	1.625	42.38	40.07
27	3	137.5	112.5	1.625	48.04	49.59
28	5	52.5	112.5	1.625	53.69	52.57
29	3	52.5	237.5	1.625	24.36	23.80
30	5	52.5	237.5	1.625	44.01	41.14

highly complex IR spectra (Fig. 1)). In the spectrum of the unloaded biomass (a) the broadband centered at 3410 cm^{-1} can be ascribed to s amino (-NH2) and to alcohol groups (-OH) stretching modes (Choy et al., 1999). The existence of amine groups is generally indicated by a shoulder at around 3265 cm^{-1} (Hall et al., 1966); however, this peak is frequently hidden by vibrations of -OH groups. The absorbance peak at 2933 cm^{-1} could be attributed to the C-H stretch (Hall et al., 1966). 23002400 cm^{-1} region is for NH_2^+, NH^+ and N-H bond of IHB. The peak at 1633 cm^{-1} refers to the carboxylate salt COO-M, where M stands for the metal cations like Na^+, K^+, Ca_2^+, and Mg_2^+ that may naturally exist in the biomass (Sa and Kutsal, 2000). The presence of carboxyl groups in the polysaccharide structure was ascertained with the strong sorption peaks between 1000 and 1100 cm^{-1} (Kleinübing et al., 2010). The absorbance peaks at 480 cm^{-1} and 810 cm^{-1} are assigned to the bending of the Si-O-Si and stretching of Si-OH, respectively (Choy et al., 1999). These peaks are indicative of silica gel (Svecova et al., 2006). The FTIR spectra of thorium-loaded biomass (b) showed that the peaks related to amino (-NH_2) and alcohol groups (-OH) band centered at 3410 cm^{-1} are shifted to 3421 cm^{-1} due to Th(IV) ions sorption. The peak of -CH bond at around 2933 cm^{-1} is shifted to 2985 cm^{-1}. The small absorption peaks at 2300-2400 cm^{-1} indicative of NH_2^+, NH^+ and N-H bond of IHB disappeared indicating that functional amino groups were involved in the sorption process. In addition, the peak of carboxyl groups (C-O) at 1092 cm^{-1} and the peak of carboxylate groups (C=O) at 1633 cm^{-1} are shifted to 1102 cm^{-1} and to 1636 cm^{-1}, respectively. These FTIR results showed that the chemical interactions between the C-H, N-H and -OH groups of IHB and the Th(IV) ions are mainly involved in the sorption metal ion onto the studied biosorbent.

3.2 Statistical analysis

The sorption process optimization was performed using the response surface methodology based on central composite design (RSM-CCD). Thus, 30 experiments were accomplished. Initial pH and initial concentration of metal ion solution ($mol.L^{-1}$), IHB dose ($g.L^{-1}$), and sorption duration (min) were selected as four independent variables that could potentially influence the sorption removal of Th(IV) ions. The experimental results based at each point on the experimental design are presented in Table 2 which depicts a close agreement between the experimental and predicted percentage sorption removal of Th(IV) by studied biomass. The obtained results were then evaluated by analysis of variance (ANOVA) to assess the goodness of fit.

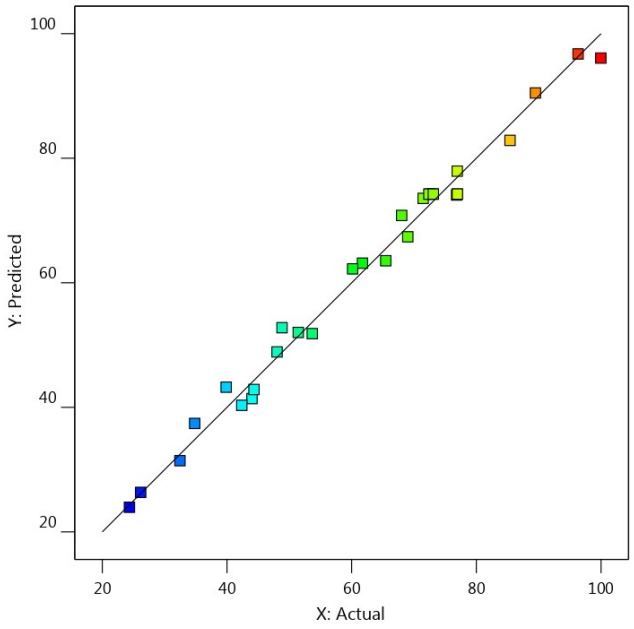

Figure 2: The plot of predicted values versus experimental (actual) values of Th(IV) ions biosorption removal.

The ANOVA of the quadratic polynomial model demonstrates that the model is highly significant as is evidenced by the calculated F-value and very low p-value (Table 3). The logarithm transform function was recommended to evaluate the investigated response. The model terms are considered significant if the p-value (value of prob. > F) is less than 0.005 (Mahmoudiani et al., 2021).

Lack-of-fit, as a special diagnostic test for the reliability of a model, formally tests how well the model fits the data. As the statistic parameter, the F-value is used to determine whether the lack of fit is significant or not, at a significant level a (Mahmoudiani et al., 2021). For Th(IV) biosorption removal, the lack-of-fit F-value of 4.49 and P-value of 0.0555 imply the lack-of-fit is not significant (Table 3). Also, considering the lack-of-fit p-value in the ANOVA table is greater or equal to 0.10, the model appears adequate. If the model does not fit well with the data, this will be significant. The insignificant lack of fit is desirable.

The goodness-of-fit of the statistical model was also estimated, by the coefficient of determination (R^2). The analysis of variance was statistically significant ($p < 0.0001$) and suggested that the variables in the model can explain the experimental variation of the sorption capacity of biosorbent for Th(IV) (Ahmad and Alrozi, 2010). The R^2 value is equal to 0.9895 or close to 1, which is desirable. The adjusted R^2 value is equal to 0.9796; it is particularly useful for comparing multi-term models. The result showed that the adjusted R^2 value is very proximate to the actual value R^2 which indicates adequate model-data fit. The results suggested that the model was good and can well depict independent factors on the response (Y). The plots of experimental (actual) and predicted values of Th(IV) biosorption removal are shown in Fig. 2. A good correlation between input and output variables is also shown by the model.

Figure 3 shows the perturbation plot for Th(IV) ions biosorption removal model. As observed from this plot, the initial pH of the solution (factor A), sorption duration (factor B), and IHB dose (factor D) have a positive effect on Th(IV) ions biosorption removal, while initial Th(IV) ion solution concentration (factor C) has a negative effect on the investigated response. According to the perturbation plot, the initial pH of the solution was determined as the most effectual factor on Th(IV) ions biosorption removal.

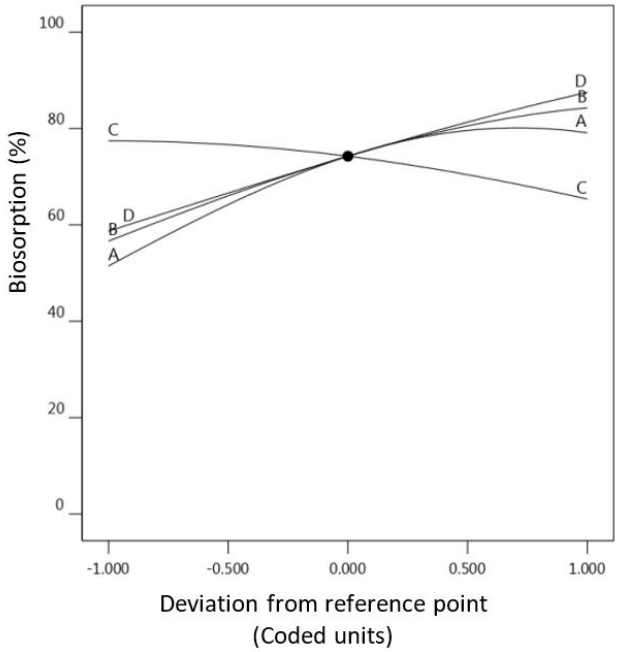

Figure 3: Perturbation plot for Th(IV) ions biosorption removal model.

3.2.1 Effect of sorption parameters on the percentage biosorption of Th(IV) ions on IHB

Using the statistical methodology, central composite response surface design, the polynomial model describing the correlation between the logarithm of percentage biosorption of Th(IV) ions on IHB, and the actual levels of the four independent variables were obtained as follows:

$$\begin{aligned} Log_{10}(\text{percentage biosorption}) &= 1.87 + 0.0933A \\ &+ 0.0863B - 0.0368C + 0.0867D - 0.0037AB \\ &+ 0.0051AC - 0.0167AD + 0.0086BC - 0.0145BD \\ &+ 0.0085CD - 0.0658A^2 - 0.0312B^2 - 0.0186C^2 \\ &- 0.0154D^2 \end{aligned}$$

According to ANOVA (Table 3), A (initial pH), B (sorption duration), C (initial Th(IV) concentration), D (IHB dose), A^2, B^2, C^2, and D^2 are more significant. However, AC, AD, BC, BD, and CD have less effect on the removal of Th(IV).

Table 3: Analysis of variance (ANOVA) for the quadratic model.

Source	Degrees of freedom	Sum of squares	Mean square	F Value	P-value/Prob. > F
Model	14	0.7450	0.0532	100.69	< 0.0001 significant
A-initial pH	1	0.2090	0.2090	395.47	< 0.0001
B-sorption duration	1	0.1789	0.1789	338.45	< 0.0001
C-initial concentration	1	0.0325	0.0325	61.52	< 0.0001
D-IHB dose	1	0.1803	0.1803	341.17	< 0.0001
AB	1	0.0002	0.0002	0.4122	0.5305
AC	1	0.0004	0.0004	0.7986	0.3856
AD	1	0.0045	0.0045	8.45	0.0108
BC	1	0.0012	0.0012	2.24	0.1550
BD	1	0.0034	0.0034	6.36	0.0235
CD	1	0.0012	0.0012	2.19	0.1595
A^2	1	0.1188	0.1188	224.78	< 0.0001
B^2	1	0.0268	0.0268	50.64	< 0.0001
C^2	1	0.0095	0.0095	18.01	0.0007
D^2	1	0.0065	0.0065	12.23	0.0032
Residual	15	0.0079	0.0005		
Lack of fit	10	0.0071	0.0007	4.49	0.0555 not significant
Pure error	5	0.0008	0.0002		
R^2	0.9895				
Adjusted R^2	0.9796				

For visualizing the relationship between the percentage biosorption of Th(IV), which is dependent variable, and the sorption removal conditions, which are independent variables, a quadratic polynomial model equation we applied to construct threedimensional surface plots (Fig. 4). Figure 4 shows the 3D plot, which depicts the combined effect of IHB dose and initial pH of solution on percentage biosorption of Th(IV) on IHB at fixed sorption duration and initial Th(IV) concentration in the aqueous solution. As can be seen from the graph, both the independent variables significantly affect the sorption removal process. Percentage biosorption of Th(IV) on IHB increases with pH ranging from 2.0 to 4.5. The reason for this is that at low pH the protonated functional groups reduce the number of binding sites of the biosorbent. In addition, at low pH the competition for surface sites between Th(IV) ions and hydrogen ions increases resulting in a decrease in sorption removal. Even so, the amount of biosorbed metal (qt), declines at pH higher than 4.5, due to the formation of different thorium species with lower sorption affinities such as $[Th_2(OH)_2]^{6+}$, $[Th3(OH)5]^{7+}$ and $[Th_4(OH)_8]^{8+}$ (Gupta and Bhattacharyya, 2011). The optimum pH for the sorption removal of Th(IV) on IHB has been found to be 4.5. Sorbent dose is another important factor regarding the sorption process because this factor determines the sorbent capacity for a given initial concentration of the sorbate (Bulut and Aydın, 2006). It is obvious from Fig. 4, by increasing the sorbent dose there is a remarkable increase in the sorption removal of Th(IV). Maximum Th(IV) sorption removal was observed at the highest level of sorbent dose (5 $g.L^{-1}$). The surface of IHB is composed of sorption sites and by increasing the biosorbent dose, higher sorption sites are available for sorption removal of Th(IV) ions.

The combined effect of sorption duration and initial Th(IV) ions solution concentration is shown in Fig. 6. It has been revealed from this study that the rate of Th(IV) removal increased due to increasing sorption duration and the curve gets equilibrium after 95 minutes. The initial rapid sorption was probably owing to the participation of characteristic functional groups and binding surface sites (Tembhurkar and Dongre, 2006). In the initial period of sorption, large numbers of unoccupied sites are available, and thereafter, repulsive forces between the already sorbed solute molecules on the sorbent surface and free solute molecules in the bulk phase, make it difficult to occupy the remaining vacuous sites. In the same way, the variation of percentage biosorption of Th(IV) with biomass dose and initial Th(IV) ions solution concentration at a fixed sorption duration of 95 minutes and initial pH of 4.5 is illustrated in Fig. 6. As may be viewed, by increasing the initial Th(IV) ions solution concentration from 50 to 300 $mg.L^{-1}$, the percentage biosorption of Th(IV) decreases. The initial Th(IV) concentration constitutes an important driving force in the mass transfer (Bouberka et al., 2006). Maximum percentage biosorption of Th(IV) was observed in the Th(IV) ions initial concentration ranging from 50 to 210 $mg.L^{-1}$ and IHB dose ranging from 3.75 to 5 $g.L^{-1}$.

According to the obtained results pH value of 4.5, initial metal ion solution concentration of 210 $mg.L^{-1}$, IHB dose of 5 $g.L^{-1}$, and sorption duration of 95 minutes were proven to be the optimum conditions, for maximum biosorption removal (≥99%) of Th(IV) ions from aqueous solutions.

3.3 Sorption kinetics

The kinetics of sorption removal is doubtless probably a very important factor in the prediction of the rate of sorption of a sorbent in a given solid-liquid system (Gupta and Bhattacharyya, 2011). The sorption kinetic data were analyzed using the pseudo-first-order model (PFO) (Lager-

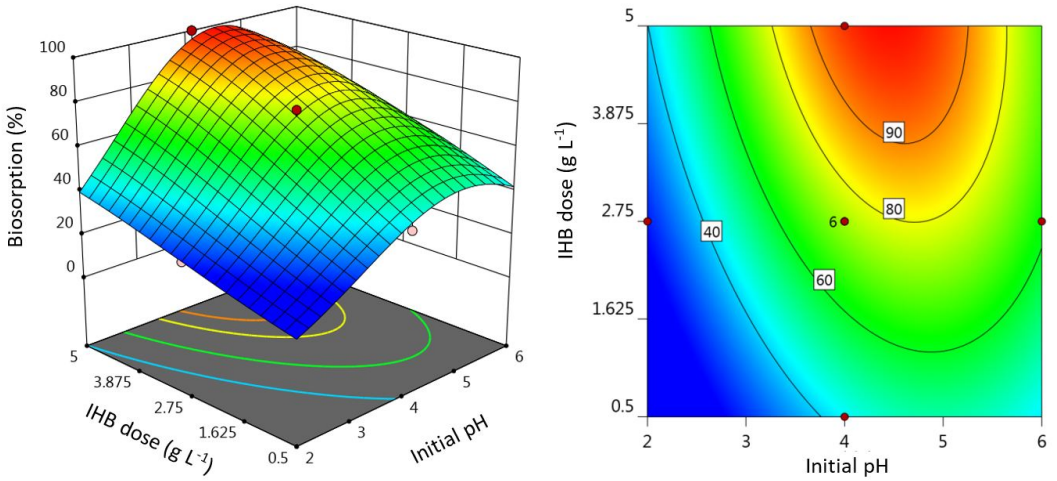

Figure 4: The combined effect of pH and sorbent dose at fixed initial concentration (175 mg.L^{-1}) and sorption duration (95 min).

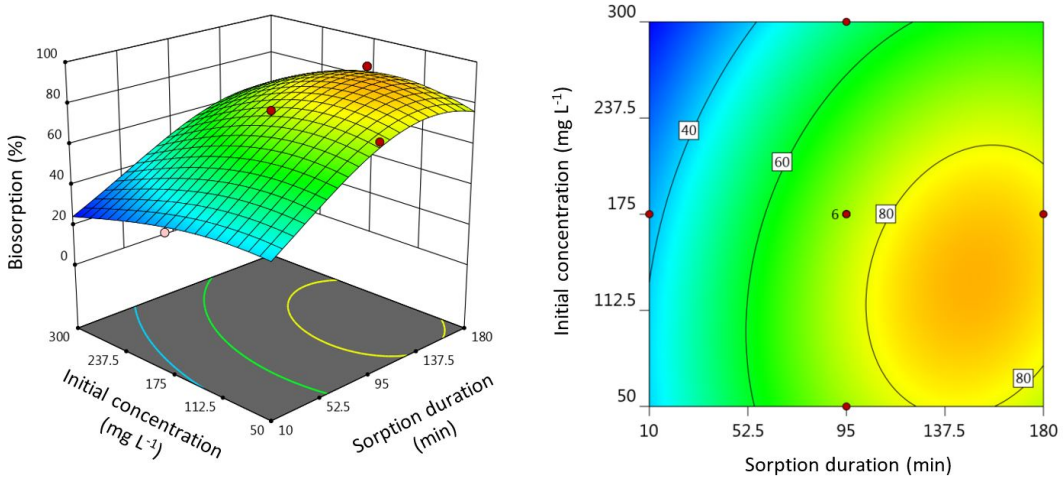

Figure 5: The combined effect of initial Th(IV) ions solution concentration and sorption duration at fixed pH (4) and sorbent dose (2.75 g.L^{-1}) on Th(IV) sorption.

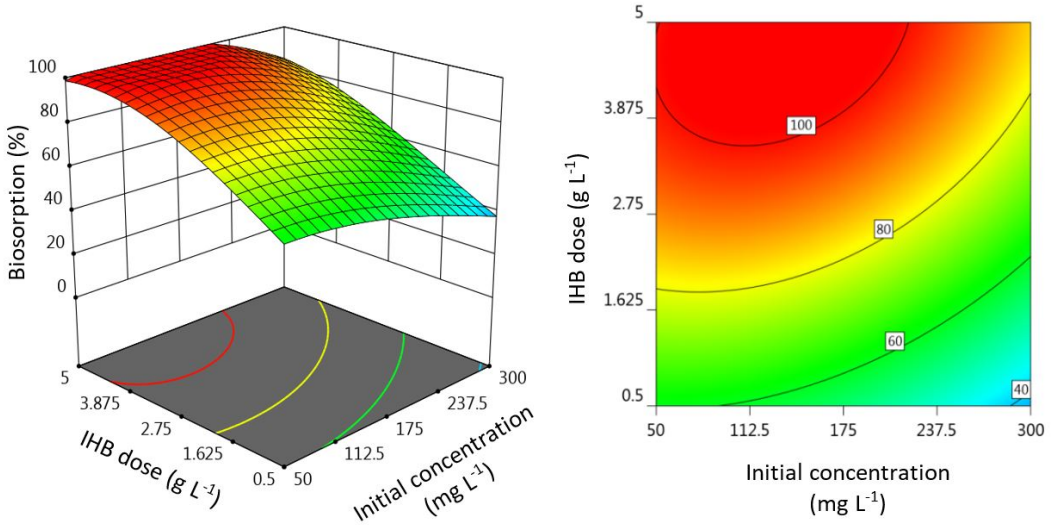

Figure 6: The combined effect of sorbent dose and initial Th(IV) ions solution concentration at fixed pH (4.5) and sorption duration (95 min).

gren, 1898), pseudo-second-order model (PSO) (Ho and McKay, 1999), and intraparticle diffusion models (Weber Jr and Morris, 1963), the experimental sorption kinetic data were estimated with the linear forms of these three models.

The PFO model assumes that the sorption process is dominated by the diffusion of sorbate at the solid-liquid phase boundary (physisorption), while the PSO model presumes that the sorption process is governed by the reaction of sorbate and the sorbent surface at the solid-liquid phase boundary (chemisorption). The essential assumption of intraparticle diffusion model is that the sorption process is controlled by the pore diffusion as well as the external mass transfer in the sorbent (Zheng et al., 2020). The equations for each kinetic model are presented below:

PFO kinetic model equation:

$$\frac{\mathrm{d}q_t}{\mathrm{d}t} = k_1(q_e - q_t) \tag{4}$$

PSO kinetic model equation:

$$\frac{\mathrm{d}q_t}{\mathrm{d}t} = k_2(q_e - q_t)^2 \tag{5}$$

Intraparticle diffusion (IPD) equation:

$$q_t = K_p t^{1/2} + C \tag{6}$$

where q_t (mg.g^{-1}) is the amount of the metal ions sorbed per unit mass of biosorbent at time t, k_1 is the equilibrium rate constant for the pseudo-first order kinetics (min^{-1}), qe is the equilibrium sorption capacity, t is the sorption duration (min), k_2 is the rate constant for the pseudo-second order kinetics (g.mg^{-1}.min^{-1}), here K_p is the intraparticle diffusion rate constant (mg.g^{-1}.min$^{-0.5}$) and C (mg.g^{-1}) is a constant that gives an idea about the thickness of the boundary layer.

In case the sorption process obeyed the pseudo-second-order model, a linear relationship exists between $(q_e - q_t)$ and sorption duration t, on a log-log plot. Similarly, log-log plot of t/q_t versus contact time t should be linear when the sorption process followed the pseudo-second-order model. In the same way, a plot of ln q_t versus (time)$^{0.5}$ yields the rate constant K_P (mg.g^{-1}.min$^{-0.5}$) as the slope of the graph when the sorption process obeyed the intraparticle diffusion model.

The pseudo-second-order model, owing to the highest recorded coefficient of determination ($R^2 > 0.9421$), generated the best fit with the sorption kinetic data for the investigated Th(IV)-IHB sorption systems, among the three kinetic models evaluated (Table 4).

Table 4: Kinetic parameters for Th(IV) sorption onto the IHB.

	Parameter	Value
Pseudo-first-order model	k_1 (min^{-1})	0.056
	q_e (mg.g^{-1})	138.31
	R^2	0.9161
Pseudo-second-order model	k_2 (g.mg^{-1}.min^{-1})	5.3×10^{-5}
	q_e (mg.g^{-1})	140.41
	R^2	0.9421
Intraparticle diffusion	K_p (mg.g^{-1}.min$^{-0.5}$)	9.54
	C (mg.g^{-1})	18.89
	R^2	0.903

Table 5: Isotherm parameters.

	Parameter	Value
Langmuir isotherm	q_{max}	142.86
	k_L	0.067
	R_L	0.02-0.1
	R^2	0.9908
Freundlich isotherm	K_F	15.88
	n	0.3587
	R^2	0.9491
Temkin isotherm	A	0.21
	B	64.056
	R^2	0.9888

3.4 Sorption isotherm models

The sorption isotherm modeling is a very essential way of identifying or predicting the mechanism of sorption processes. As well, biosorption isotherms can be used for the determination of the solid/liquid partition coefficients (K_d). The Langmuir sorption isotherm is applicable to sorption processes that occur on homogeneous surfaces with sorption sites having different activities (Langmuir, 1918), while the Freundlich isotherm model presumes that sorption occurs on a heterogeneous surface having sites with different energies of sorption (Freundlich et al., 1906). The Temkin isotherm model predicts the heat of sorption, and the sorbate-sorbent interaction on a surface (Temkin and Pyzhev, 1940). The linear forms of the aforementioned isotherms are given as:

$$\frac{C_e}{q_e} = \frac{1}{k_L q_m} + \frac{C_e}{q_m} \tag{7}$$

here q_m (mg.g^{-1}) and k_L are the maximum sorption capacity and the Langmuir constant, and C_e (mg.L^{-1}) is the sorbate solution concentration at equilibrium.

$$\mathrm{Ln}\, q_e = \mathrm{Ln}\, k_F + \frac{1}{n}\mathrm{Ln}\, C_e \tag{8}$$

where K_F (mg.g^{-1}) is the Freundlich constant and n is the Freundlich exponent related to the sorption capacity and sorption intensity respectively. The values of $n > 1.0$ indicate that the sorption of Th(IV) ions onto IHB is favorable (Talebi et al., 2017).

$$q_e = B\mathrm{Ln}\, A_T C_e \tag{9}$$

in which A_T is the Temkin isotherm equilibrium binding constant (L.g^{-1}) and $B = (RT)/b$, in which b is the Temkin isotherm constant related to the heats of sorption, R is the universal gas constant (8.314 J.mol^{-1}.K^{-1}) and T is the temperature (K).

The values of corresponding isotherm parameters and their correlation coefficients (R^2) are presented in Table 5.

High R^2 is derived by fitting experimental data into the Langmuir isotherm model ($R^2 > 0.990$) and the Temkin isotherm model ($R^2 > 0.989$), as compared with the Freundlich isotherm model ($R^2 > 0.858$). The Langmuir

maximum monolayer adsorption capacity was found to be 142.86 mg.g^{-1}.

Additional to the important characteristics of the Langmuir isotherm, another parameter referred to separation factor or equilibrium parameter, R_L, is calculated as follows (Hall et al., 1966):

$$R_L = \frac{1}{1 + K_{LC_0}} \tag{10}$$

here, K_L (L.mg^{-1}) is the Langmuir constant and C_0 (mg.L^{-1}) is the initial Th(IV) ions solution concentration. The value of R_L specifies the shape of the isotherms to be either unfavorable ($R_L > 1$), linearly favorable ($R_L = 1$), favorable ($0 < R_L < 1$), or irreversible ($R_L = 0$).

3.5 Sorption thermodynamics

The effect of temperature on the sorption of thorium ions on IHB was investigated. Sorption removal analysis for thorium was conducted under various temperatures that ranged from 298 K to 318 K (25 °C to 45 °C). In all cases, the IHB dose 1.63 g.L^{-1}, the initial pH of the solution 4.5, and the sorption duration was 137.5 min. As a result, it was found that metal ion sorption for IHB increased when the temperature increased from 298 K to 318 K (Fig. 7). This is mostly the result of the increase in surface activity suggesting that sorption between Th(IV) ions and IHB is an endothermic process. This shows that sorption affinity and capacity tend to increase when the temperature increases. As the temperature of a solution increased, the mobility of the ions in the solution also increased, and consequently the collision frequency between the solute and sorbent surface became higher, thus increasing sorption.

To investigate the thermodynamic nature of IHB for Th(IV) ions sorption, different parameters viz. Gibbs free energy ($\Delta G°$), enthalpy change ($\Delta H°$), and entropy change ($\Delta S°$) were calculated using the following equations:

$$\Delta G° = -RT\mathrm{Ln}\,(K_c) \tag{11}$$

where K_C is the sorption equilibrium constant calculated as the ratio of amount of sorbed sorbate (q_e) to the sorbate amount remaining in the solution (C_e):

$$K_c = \frac{q_e}{C_e} \tag{12}$$

The temperature dependence of the equilibrium constant of a chemical reaction is correctly described by the well-known van't Hoff equation:

$$\mathrm{Ln}\,(K_c) = \frac{\Delta S°}{R} - \frac{\Delta H°}{RT} \tag{13}$$

The thermodynamic parameters of $\Delta H°$ and $\Delta S°$ for the sorption of Th(IV) ions on IHB were determined respectively from the slope and intercept of the plot of Ln (K_c) versus $1/T$ (van't Hoff plot) in Fig. 8. The calculated thermodynamic parameters are illustrated in Table 6. $\Delta H°$ value of 7.358 kJ.mol^{-1} indicated that the sorption removal of Th(IV) ions by IHB was an endothermic process and the sorption efficiency will increase with increasing temperature. Generally, the sorption of gas on the surface of a solid leads to a decrease in entropy. But for the complicated system of sorption from solution may not be the same. The positive value of entropy (0.0347 J.K^1.mol^1) ascribed that more randomness existed during the sorption process and the process was said to be entropy-driven (Nayak and Devi, 2020). It also suggests a certain affinity of the sorbent with thorium. However, the low value of $\Delta S°$ might connote that no remarkable change in entropy occurs during the biosorption of Th(IV) by the IHB. Negative $\Delta G°$ (-2.955 kJ.mol^{-1}) depicted that the forward reaction is favored and there are more products than reactants. What's more, the larger the value of ΔG, the more product-favored the reaction will be. It is well-known that the absolute magnitude of the change in free energy for physisorption generally ranges from -20 kJ.mol^{-1} to 0 kJ.mol^{-1} and for chemisorption the corresponding change lies in the range of -80 kJ.mol^{-1} to 400 kJ.mol^1 (Aksu, 2002). The deduced values of the ΔG suggested that the biosorption process of Th(IV) ions onto studied immobilized hybrid biosorbent occurred via the physisorption process. Essentially, the heat developed in physical sorption is very close to that of condensation, i.e., 2.1 to 20.9 kJ.mol^{-1} (Aksu, 2002), while the heat of chemisorption normally lie in the range of 80 to 200 kJ.mol^{-1} (Gueu et al., 2007). Therefore, the calculated $\Delta H°$ value (7.385 kJ.mol^{-1}) confirmed the occurrence of physical sorption.

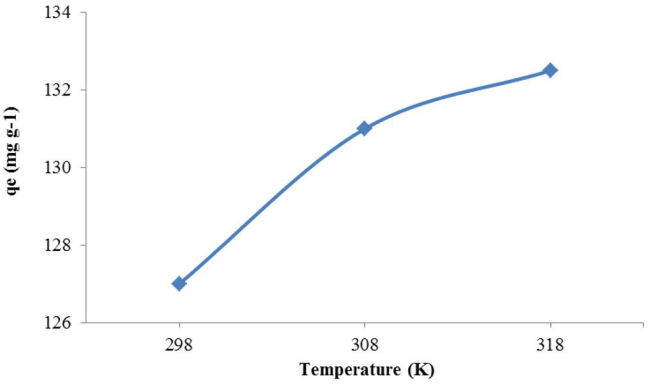

Figure 7: Temperature dependence of sorption capacity of IHB for Th(IV) ions.

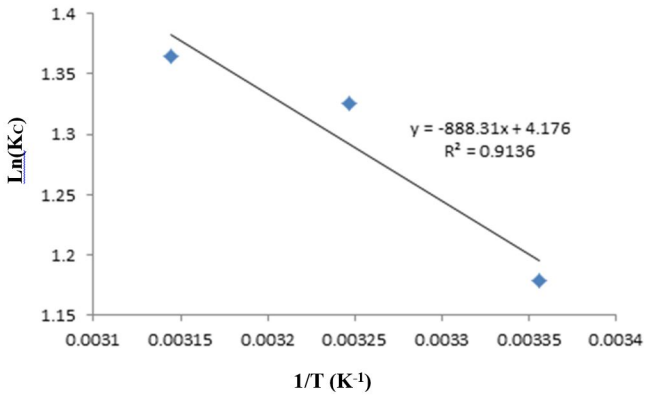

Figure 8: Vant Hoff plot for the thorium sorption on IHB.

Table 6: The obtained thermodynamic parameters for Th(IV) ions sorption onto IHB in aqueous solution.

	ΔS° (kJ.mol^{-1})	ΔS° (J.mol^1.K^{-1})	ΔG (kJ.mol^{-1})		
			298K	308K	318K
IHB-Th(IV)	7.385	0.0347	-2.955	-3.302	-3.649

4 Conclusion

The removal of thorium ions from aqueous solutions was accomplished using biosorption techniques. An immobilized hybrid biosorbent (IHB) was developed and applied to remove thorium ions from the aqueous solution. The obtained results showed that IHB can be effectively used for thorium removal from aqueous solutions. In this study, the statistical methodology, central composite response surface design is demonstrated to be effective and reliable in ascertaining the optimal conditions for the sorption removal of thorium ions onto as developed IHB. From batch experiments, conducted as designed by central composite experimental design, the biosorption percentage was greatly dependent on operational variables such as initial pH of the solution, initial Th(IV) ions solution concentration, sorption duration, and biosorbent dose, as evidenced by the response surface 3D plots. In the equilibrium study, the experimental data showed that the sorption process fits with various isotherms in the following order Langmuir > Temkin> Freundlich. Thus, IHB could be utilized as a novel, low-cost, efficient adsorbent for the sorption removal of thorium. The maximum monolayer sorption capacity estimated by the Langmuir model was 142.86 mg.g^1. Time-dependent investigations disclosed that the adsorption process pursues the pseudo-second-order kinetic model via the pore diffusion mechanism. Thermodynamic parameters have also been appraised, and the results depicted that the overall sorption process is physisorption, entropy-driven, endothermic in nature, and the forward reaction is favored.

References

Ahmad, M. A. and Alrozi, R. (2010). Optimization of preparation conditions for mangosteen peel-based activated carbons for the removal of Remazol Brilliant Blue R using response surface methodology. *Chemical Engineering Journal*, 165(3):883–890.

Akar, T., Kaynak, Z., Ulusoy, S., et al. (2009). Enhanced biosorption of nickel (II) ions by silica-gel-immobilized waste biomass: biosorption characteristics in batch and dynamic flow mode. *Journal of Hazardous Materials*, 163(2-3):1134–1141.

Aksu, Z. (2002). Determination of the equilibrium, kinetic and thermodynamic parameters of the batch biosorption of nickel (II) ions onto Chlorella vulgaris. *Process Biochemistry*, 38(1):89–99.

Bağ, H., Lale, M., and Türker, A. R. (1998). Determination of iron and nickel by flame atomic absorption spectrophotometry after preconcentration on saccharomyces cerevisiae immobilized sepiolite. *Talanta*, 47(3):689–696.

Bayyari, M., Nazal, M., and Khalili, F. (2010). The effect of ionic strength on the extraction of Thorium (IV) from nitrate solution by didodecylphosphoric acid (HDDPA). *Journal of Saudi Chemical Society*, 14(3):311–315.

Bouberka, Z., Khenifi, A., Benderdouche, N., et al. (2006). Removal of Supranol Yellow 4GL by adsorption onto Cr-intercalated montmorillonite. *Journal of Hazardous Materials*, 133(1-3):154–161.

Bulut, Y. and Aydın, H. (2006). A kinetics and thermodynamics study of methylene blue adsorption on wheat shells. *Desalination*, 194(1-3):259–267.

Choppin, G. R. (2003). Actinide speciation in the environment. *Radiochimica Acta*, 91(11):645–650.

Choy, K. K., McKay, G., and Porter, J. F. (1999). Sorption of acid dyes from effluents using activated carbon. *Resources, Conservation and Recycling*, 27(1-2):57–71.

Donat, R. and Aytas, S. (2005). Adsorption and thermodynamic behavior of uranium (VI) on Ulva sp.-Na bentonite composite adsorbent. *Journal of Radioanalytical and Nuclear Chemistry*, 265(1):107–114.

Freundlich, H. et al. (1906). Over the adsorption in solution. *J. Phys. chem*, 57(385471):1100–1107.

Guerra, D. L., Viana, R. R., and Airoldi, C. (2009). Adsorption of thorium (IV) on chemically modified Amazon clays. *Journal of the Brazilian Chemical Society*, 20(6):1164–1174.

Gueu, S., Yao, B., Adouby, K., et al. (2007). Kinetics and thermodynamics study of lead adsorption on to activated carbons from coconut and seed hull of the palm tree. *International Journal of Environmental Science & Technology*, 4(1):11–17.

Gupta, S. S. and Bhattacharyya, K. G. (2011). Kinetics of adsorption of metal ions on inorganic materials: a review. *Advances in Colloid and Interface Science*, 162(1-2):39–58.

Gusain, D., Bux, F., and Sharma, Y. C. (2014). Abatement of chromium by adsorption on nanocrystalline zirconia using response surface methodology. *Journal of Molecular Liquids*, 197:131–141.

Hall, K. R., Eagleton, L. C., Acrivos, A., et al. (1966). Pore-and solid-diffusion kinetics in fixed-bed adsorption under constant-pattern conditions. *Industrial & Engineering Chemistry Fundamentals*, 5(2):212–223.

He, Q., Chang, X., Wu, Q., et al. (2007). Synthesis and applications of surface-grafted Th (IV)-imprinted polymers for selective solid-phase extraction of thorium (IV). *Analytica Chimica Acta*, 605(2):192–197.

Herring, J. S., MacDonald, P. E., Weaver, K. D., et al. (2001). Low cost, proliferation resistant, uranium–thorium dioxide fuels for light water reactors. *Nuclear Engineering and Design*, 203(1):65–85.

Ho, Y.-S. and McKay, G. (1999). Pseudo-second order model for sorption processes. *Process biochemistry*, 34(5):451–465.

Hrenovic, J., Milenkovic, J., Daneu, N., et al. (2012). Antimicrobial activity of metal oxide nanoparticles supported onto natural clinoptilolite. *Chemosphere*, 88(9):1103–1107.

Ilaiyaraja, P., Deb, A. K. S., and Ponraju, D. (2015). Removal of uranium and thorium from aqueous solution by ultrafiltration (UF) and PAMAM dendrimer assisted ultrafiltration (DAUF). *Journal of Radioanalytical and Nuclear Chemistry*, 303(1):441–450.

James, D., Venkateswaran, G., and Rao, T. P. (2009). Removal of uranium from mining industry feed simulant solutions using trapped amidoxime functionality within a mesoporous imprinted polymer material. *Microporous and Mesoporous Materials*, 119(1-3):165–170.

Janin, A., Zaviska, F., Drogui, P., et al. (2009). Selective recovery of metals in leachate from chromated copper arsenate treated wastes using electrochemical technology and chemical precipitation. *Hydrometallurgy*, 96(4):318–326.

Kiliari, T. and Pashalidis, I. (2011). Thorium determination in aqueous solutions after separation by ion-exchange and liquid extraction. *Journal of Radioanalytical and Nuclear Chemistry*, 288(3):753–758.

Kimura, T. and Kobayashi, Y. (1985). Coprecipitation of uranium and thorium with barium sulfate. *Journal of radioanalytical and nuclear chemistry*, 91(1):59–65.

Kleinübing, S. J., Vieira, R. S., Beppu, M. M., et al. (2010). Characterization and evaluation of copper and nickel biosorption on acidic algae Sargassum filipendula. *Materials Research*, 13(4):541–550.

Lagergren, S. K. (1898). About the theory of so-called adsorption of soluble substances. *Sven. Vetenskapsakad. Handingarl*, 24:1–39.

Langmuir, I. (1918). The adsorption of gases on plane surfaces of glass, mica and platinum. *Journal of the American Chemical society*, 40(9):1361–1403.

Mahan, C. A. and Holcombe, J. A. (1992). Immobilization of algae cells on silica gel and their characterization for trace metal preconcentration. *Analytical Chemistry*, 64(17):1933–1939.

Mahmoudiani, F., Milani, S. A., Hormozi, F., et al. (2021). Application of response surface methodology for modeling and optimization of the extraction and separation of Se (IV) and Te (IV) from nitric acid solution by Cyanex 301 extractant. *Progress in Nuclear Energy*, page 104052.

Mungasavalli, D. P., Viraraghavan, T., and Jin, Y.-C. (2007). Biosorption of chromium from aqueous solutions by pretreated aspergillus niger: batch and column studies. *Colloids and Surfaces A: Physicochemical and Engineering Aspects*, 301(1-3):214–223.

Nayak, S. and Devi, N. (2020). Studies on the solvent extraction of indium (III) from aqueous chloride medium using Cyphos IL 104. *Materials Today: Proceedings*, 30:258–261.

Niedzielski, P. and Siepak, M. (2003). Analytical methods for determining arsenic, antimony and selenium in environmental samples. *Polish Journal of Environmental Studies*, 12(6).

Petrus, R. and Warchoł, J. (2003). Ion exchange equilibria between clinoptilolite and aqueous solutions of Na+/Cu2+, Na+/Cd2+ and Na+/Pb2+. *Microporous and Mesoporous Materials*, 61(1-3):137–146.

Sa, Y. and Kutsal, T. (2000). Determination of the biosorption heats of heavy metal ions on Zoogloea ramigera and Rhizopus arrhizus. *Biochemical Engineering Journal*, 6(2):145–151.

Srinath, T., Verma, T., Ramteke, P., et al. (2002). Chromium (VI) biosorption and bioaccumulation by chromate resistant bacteria. *Chemosphere*, 48(4):427–435.

Svecova, L., Spanelova, M., Kubal, M., et al. (2006). Cadmium, lead and mercury biosorption on waste fungal biomass issued from fermentation industry. I. Equilibrium studies. *Separation and Purification Technology*, 52(1):142–153.

Talebi, M., Abbasizadeh, S., and Keshtkar, A. R. (2017). Evaluation of single and simultaneous thorium and uranium sorption from water systems by an electrospun PVA/SA/PEO/HZSM5 nanofiber. *Process Safety and Environmental Protection*, 109:340–356.

Tembhurkar, A. and Dongre, S. (2006). Studies on fluoride removal using adsorption process. *Journal of Environmental Science & Eengineering*, 48(3):151–156.

Temkin, M. and Pyzhev, V. (1940). Recent modifications to Langmuir isotherms.

Wahab, R., Kim, Y.-S., and Shin, H.-S. (2009). Synthesis, characterization and effect of pH variation on zinc oxide nanostructures. *Materials Transactions*, 50(8):2092–2097.

Weber Jr, W. J. and Morris, J. C. (1963). Kinetics of adsorption on carbon from solution. *Journal of the Sanitary Engineering Division*, 89(2):31–59.

Zheng, A. L. T., Phromsatit, T., Boonyuen, S., et al. (2020). Synthesis of silver nanoparticles/porphyrin/reduced graphene oxide hydrogel as dye adsorbent for wastewater treatment. *FlatChem*, 23:100174.